Sound velocity and absorption in a coarsening foam

Nicolás Mujica* and Stéphan Fauve
Laboratoire de Physique Statistique, Ecole Normale Supérieure, 24 rue Lhomond, 75231 Paris Cedex 05, France
(Received 10 December 2001; revised manuscript received 4 June 2002; published 19 August 2002)

We present experimental measurements of sound velocity and absorption in a commercial shaving foam. We observe that both quantities evolve with time as the foam coarsens increasing its mean bubble radius $\langle R\rangle$. By varying the acoustic frequency we probe the foam from the large wavelength regime, $\lambda \approx 1500\langle R\rangle$, down to the scale $\lambda \approx 20\langle R\rangle$. Sound absorption α varies significantly with both the foam age and the excitation frequency. After an initial transition time of 20 min, the attenuation per wavelength, $\alpha\lambda$, varies linearly with the foam age. In addition, for evolution times smaller than ≈ 90 min, we observe that $\alpha\lambda$ scales linearly with both foam age and frequency. From these scalings we show that the thermal dissipation mechanism is the dominant one. Sound velocity c is initially frequency independent but the medium becomes slightly dispersive as the foam coarsens. We observe that sound velocity depends on the evolution of the structure of the foam, even in the large wavelength regime. After 2 h of foam coarsening, c decreases at least by a factor of 20%, due to the softening of the foam. These facts are explained by considering the liquid matrix elasticity, due to the presence of surfactant molecules. A simple model of foam structure, combined with results of Biot's theory for porous media, gives both good qualitative and quantitative agreement with our experimental results in the low frequency regime.

DOI: 10.1103/PhysRevE.66.021404 PACS number(s): 82.70.Rr, 43.20.+g

I. INTRODUCTION

Sound propagation through bubbly liquids has attracted much attention, from both theoretical [1–5] and experimental points of view [6–10]. The presence of gas bubbles in a liquid profoundly affects its acoustic properties. For example, a common feature of bubbly liquids is the very low speed of sound that can be reached, even at very small gas volume fractions. In general, the effective sound speed c_{eff} can be lower than both the speed in the pure liquid c_l and in the pure gas c_g. This reduction is in fact due to the high contrast of acoustic properties of both media. More precisely, the density of the mixture is dominated by the density of the liquid and its compressibility is given by that of the gas, thus a lower effective sound velocity is expected.

It is also known that liquids containing a small amount of gas bubbles possess a relatively high sound attenuation compared to the gas-free liquid [11,12]. The sound wave damping is mainly due to three mechanisms, namely, the viscosity of the surrounding liquid, the gas thermal conductivity, and the scattering of sound by the bubble [11–14]. We note that the last mechanism is not a dissipative phenomenon, but it effectively removes energy from the incident sound wave, reemitting it in other directions than the incident one.

Most of theoretical and experimental studies on sound propagation in bubbly liquids deal with the limit of very small gas volume fraction $\phi \ll 1$. In addition, theoretical models generally assume that the acoustic wavelength is much larger than the typical bubble size. Commander and Prosperetti [10] give an extensive review of the subject and show the validity of an effective-medium approach (the van Wijngaarden–Papanicolaou model [1,4,5]) by comparison with the experimental data available at the time. They conclude that the quoted model is valid for acoustic frequencies ω much smaller than the bubble resonant frequency ω_{r}. Even at gas volume fractions of the order of 5×10^{-4}, discrepancies between the experimental and theoretical values of sound attenuation were found for $\omega \approx \omega_{\mathrm{r}}$. They offer as explanation the fact that at resonance the scattering cross section of a single bubble increases dramatically, then breaking down the assumption that the bubbles do not interact. The problem of the effect of bubble interactions on the sound propagation has been theoretically studied only recently, both at low [15] and high gas volume fractions [16]. An interesting prediction of these theoretical studies is that the sound velocity is found to increase with respect to the noninteracting effective-medium result [15,16], but almost no experimental work has been carried out to test this result.

If we increase ϕ enough, bubbles will eventually come in contact, producing a foam. Contrary to bubbly liquids of small gas volume fraction, very little work has been done on sound propagation through foams. From an experimental point of view we believe that this is due to the high absorption of acoustic waves in these systems, which makes acoustic measurements a difficult task. Another possible reason is the difficulty in obtaining reproductive bubble distributions, a problem also found in the experiments concerning low bubble concentrations [10]. However, some interesting experimental results were obtained by Orenbakh and Shushkov [17], who present an attempt of verification of the dependence of the effective sound velocity c on the gas volume fraction ϕ [as given by Eq. (2) of Sec. I B]. For $\phi \approx 0.95$ they measured $c \approx 50$ m/s, which is of the order of our measured values. In addition, they measured the sound attenuation coefficient α; for acoustic frequencies between 1 and 3 kHz they found that it varies from 1 to 5 m^{-1}. Another interesting work is the study of shear wave propagation by

*Permanent address: Departamento de Física, Facultad de Ciencias Físicas y Matemáticas, Universidad de Chile, Avenida Blanco Encalada 2008, Santiago, Chile.

Sun *et al.* [18], where a much lower velocity $c \approx 3$ m/s was reported. The difference in magnitude between the compressional and shear velocities shows that a foam is much easier to shear than to compress. Concerning theoretical studies, Gol'dfarb and co-workers have studied the heat transfer effect on the absorption of sound in foams [19,20]. We note that they neglect the heat transfer between bubbles, thus neglecting thermal interactions. In Ref. [20] they also review the experimental results known at the time and they compare them with their theory. Concerning the ϕ dependence of c, the situation seems somewhat confusing, as they present some experimental results in agreement with their prediction and some others in disagreement. In general, the few experimental results that they were aware of seem to indicate that c is higher than the predicted value given by a simple effective-medium approach, the difference varying from 10% to 50%.

In this work we present an experimental study of sound propagation through a coarsening shaving foam (Gillette regular [21]). We study the aging and the frequency dependence of acoustic propagation. In particular, we show that sound velocity and absorption are quantities that evolve in time. As the mean bubble radius grows by coarsening and by varying the acoustic frequency, we are then able to vary the acoustic wavelength λ from the large wavelength regime, $\lambda \approx 1500\langle R \rangle$, down to $\lambda \approx 20\langle R \rangle$, where $\langle R \rangle$ is the mean bubble radius. In the later regime either dissipative effects or multiple scattering effects and bubble interactions are expected to become important. From the dependence of the sound absorption on both time and sound frequency we can also identify the dominant damping mechanism as the thermal dissipation. Finally, we also address in this paper the question of the theoretical prediction of the sound speed in a foam and the mechanism that explains its evolution, namely, the liquid matrix elasticity due to the presence of surfactant molecules. To our knowledge, this is the first experimental study of the acoustic properties of a coarsening foam.

This paper is organized as follows: we first review some general characteristics of aqueous foams in Sec. I A and the theoretical treatments of sound propagation through bubbly liquids in Sec. I B. The experimental setup and the acoustic measurement methods are presented in Sec. II. We then present our experimental results in Sec. III and we show how the foam coarsening is probed by acoustic measurements. Finally, a discussion of our results and the conclusions are given in Sec. IV.

A. Aqueous foams

Aqueous foams are diphasic systems with a high concentration of gas bubbles in a liquid matrix of small volume fraction, thus $\phi \lesssim 1$. In general, surfactant molecules are present in the liquid in order to decrease the bubble surface tension (reducing then the energy required to form a bubble) and to increase the stability of the liquid films.

An important characteristic of foams is that they are never in equilibrium. They are intrinsically unstable and evolve in time. Three aging mechanisms can be identified: (i) the liquid can drain due to gravity, imposing density gradients in the sample; (ii) the films that separate bubbles can become too thin and, in consequence, unstable, causing their rupture and the coalescence of adjacent bubbles; (iii) the bubble volume can vary due to gas diffusion through the liquid films due to Laplace pressure differences. In foams of high concentration of bubbles, i.e., of high gas volume fraction, there are large viscous forces that oppose the fluid drainage. In fact, polymers are generally added to the liquid to increase its viscosity, thus mechanism (i) can be very slow. Also, if surfactants are added to the liquid, the bubble interfaces are very stable under coalescence processes, so mechanism (ii) is negligible too. As in most foams the bubble size distribution is random, so process (iii) cannot be eliminated and it always occurs. Nevertheless, gases of poor solubility and poor diffusivity can be used to minimize coarsening. Thus, under certain conditions, the dominant aging mechanism is the gas diffusion between bubbles. This is indeed the case in shaving foams, as it has been shown experimentally [22,23].

When the coarsening process is due to interbubble gas diffusion, experiments have shown that foams reach a scaling state [22–24]. This means that the foam structure is dominated by the time evolution of a single length scale, which can be the radius mean value $\langle R(t) \rangle$ (the average is performed over a given bubble configuration). More precisely, this means that if we rescale the bubble radius by this time-dependent length, then the bubble size distribution becomes asymptotically time independent. As a consequence of this scaling state, it has been shown that the mean bubble radius follows a parabolic law of the form [25]

$$\langle R(t) \rangle^2 - \langle R(t_o) \rangle^2 \approx A(t - t_o), \tag{1}$$

where t_o is an arbitrary reference time and A is a constant. Previous experiments on shaving foams give $\langle R(t) \rangle \approx 15$, 30, and 50 μm for $t \approx 20$, 120, and 480 min [22,23]. In practice, the parabolic law is used to test if the foam has reached a scaling state or not.

Nevertheless, some attention should be drawn to the foam density evolution due to drainage. Experimental observations on Gillette regular samples, of ≈ 7 cm height, show that the average gas volume fraction remains constant for the first 2 h of foam aging [23]. At later times, ϕ is seen to increase slowly and a density gradient appears in the sample (ϕ increases more rapidly at the higher part of the sample). After 4 and 8 h, the spatial average of ϕ increases by a factor of 0.5% and 1%, respectively (the spatial average is taken over two measurements, at 1.5 and 5 cm above the bottom of the vessel). Thus, over the same time scales, the average density decreases by factors of $\sim 7\%$ and $\sim 14\%$, respectively. Such relatively small changes in ϕ are crucial to the density changes, which can indeed affect the foam acoustic properties. It must be noticed that as drainage depends on the foam sample geometry, in particular, on its height, these numbers are not universal. However, they agree in order of magnitude with the density changes of our own foam samples.

B. Theoretical aspects of sound propagation in bubbly liquids

This section consists in a review of the most important aspects of sound propagation through bubbly liquids in the

limit $\phi \ll 1$. Nevertheless, we note that the very definition of the effective sound speed does not depend on this limit.

The most simple effective-medium approach states that when the wavelength is much larger than the scale of the inhomogeneties, the wave propagation does not depend on the fine details of the mixture. The wave then probes an effective homogeneous medium with average acoustic properties [1,4,5,10]. Thus, for a liquid/gas mixture we can write for the effective sound speed,

$$c_{\mathrm{eff}}^2 = \frac{1}{\langle \rho \rangle \langle \chi \rangle}, \tag{2}$$

where $\langle \rho \rangle = \phi \rho_g + (1-\phi)\rho_l$ and $\langle \chi \rangle = \phi \chi_g + (1-\phi)\chi_l$ are the average density and the average compressibility, respectively. We note that this definition is quite general, in the sense that it is used for different kinds of diphasic systems, such as suspensions, emulsions, and bubbly liquids. It was apparently first written by Wood [26] and Herzfeld [27], and is often referred as Wood's formula. In this simple model, the system is characterized by the knowledge of the macroscopic quantity ϕ, and no details on the statistical bubble distribution are needed.

In the case of bubbly liquids, $\rho_l \gg \rho_g$ and $\chi_l \ll \chi_g$, and Eq. (2) takes the approximated form

$$c_{\mathrm{eff}}^2 \approx \frac{1}{\rho_l \chi_g (1-\phi)\phi}. \tag{3}$$

We note that this expression implicitly assumes that the liquid and the bubbles move with the same velocity throughout the acoustic wave. This is indeed the case at low acoustic frequencies, when the viscous boundary layer is much larger than the bubble size, $\nu_l/\omega \gg R^2$ ($\nu_l = \mu_l/\rho_l$ is the liquid kinematic viscosity, ω is the acoustic angular frequency, and R is the typical bubble size). In this case viscous forces dominate over dynamic forces and the bubbles are driven by the liquid. This was noted by Crespo [2], who also showed that in the opposite limit, $\nu_l/\omega \ll R^2$, Eq. (3) must be replaced by

$$c_{\mathrm{eff}}^2 \approx \frac{1+2\phi}{\rho_l \chi_g (1-\phi)\phi}. \tag{4}$$

Thus, if bubbles move with respect to the liquid, sound waves propagate faster.

None of the above expressions of c_{eff} take into account the structure of the bubbly liquid, thus the statistics of the bubble distribution do not play any role. In addition, sound attenuation is discarded. To go a step further, one has to take into account the fact that a bubble in a sound field behaves as a forced harmonic oscillator, its stiffness being given by the gas compressibility and the inertia by the liquid density. For an isolated bubble that undergoes adiabatic radial oscillations, the angular resonance frequency is given by [28]

$$\omega_{\mathrm{r}}^2 = \frac{3\gamma P_o}{\rho_l R^2}, \tag{5}$$

where P_o is the ambient pressure and γ is the specific heat ratio. This expression can be understood as follows: a gas bubble that undergoes adiabatic compressions has a *stiffness* of order $\gamma P_o R$ and a *radiation mass* of order $\rho_l R^3$, thus the natural frequency scales like $\sqrt{\gamma P_o/\rho_l R^2}$. For an air bubble of radius $R \approx 10\ \mu$m in water, the resonance frequency is $\omega_{\mathrm{r}}/2\pi \approx 325$ kHz. It is interesting to note that at resonance, the associated acoustic wavelength is much larger than the bubble size, $\lambda_r = 2\pi c_l/\omega_{\mathrm{r}} \approx 4.5$ mm. In addition, for small bubbles, we must take into account surface tension effects. We then replace in the above expression $P_o \to P_o + 2\sigma/R$, where σ is the liquid/gas surface tension.

A more elaborated effective-medium approach, the van Wijngaarden-Papanicolaou model [10], gives the following dispersion relation for the complex wave number k in the low gas volume fraction limit $\phi \ll 1$:

$$k^2 = \frac{\omega^2}{c_l^2} + 4\pi\omega^2 \int_0^\infty \frac{RF(R)dR}{\omega_{\mathrm{r}}^2 - \omega^2 - 2ib\omega}, \tag{6}$$

where ω is the acoustic pulsation, $F(R)$ is the normalized bubble size distribution function, and b is the damping constant (note that in spite of its name, b is a function of R and ω). This dispersion relation is analogous to the complex index of refraction of dilute gases and ''nondense'' dielectric materials [29]. In a bubbly liquid, b involves three contributions, viscous and thermal dissipation mechanisms and sound scattering, $b = b_{\mathrm{v}} + b_{\mathrm{th}} + b_{\mathrm{sc}}$ [11–14]. The phase velocity c and the absorption α are, therefore, defined as

$$c = \frac{\omega}{\mathrm{Re}[k(\omega)]}, \quad \alpha = \mathrm{Im}[k(\omega)]. \tag{7}$$

This effective-medium approach has the advantage that it provides an explicit form for the damping constant b [10]. It is interesting to note that the dispersion relation (6) can also be obtained by a multiple scattering approach for the coherent part of the acoustic wave [4,6], but in this case b is introduced by hand.

Concerning the validity of this dispersion relation, we remark that when $\omega \ll \omega_{\mathrm{r}}$ and $\phi \ll 1$, such that scattering effects are small, there is a good agreement between the values of c and α predicted by Eq. (6) and those obtained experimentally [10]. Only for wide bubble size distributions [7] and for two-dimensional bubble screens [8], the agreement can be extended to a wider range of frequencies, up to $\omega \gtrsim \omega_{\mathrm{r}}$ [10].

A final remark concerning the dispersion relation (6): if we define $\chi_g = 1/\gamma P_o$ and use the definition

$$\phi = \frac{4\pi}{3} \int_0^\infty R^3 F(R) dR, \tag{8}$$

it is easy to show that for $F(R') = n\delta(R'-R)$ and small dissipation, such that $b\omega \ll \omega_{\mathrm{r}}^2$, and considering the leading order terms in $\omega/\omega_{\mathrm{r}} \ll 1$, $\phi \ll 1$, and $c_{\mathrm{eff}}/c_l \ll 1$, the dispersion relation (6) becomes

$$k=\frac{\omega}{c_{\text{eff}}}\left(1+\frac{i}{2}\delta\right), \tag{9}$$

where $\delta=2b\omega/\omega_{\text{r}}^2$ is the dimensionless damping constant and c_{eff} is given by Eq. (3) up to order ϕ. From Eq. (7) we also obtain $c=c_{\text{eff}}$ and $\alpha=\omega\delta/(2c_{\text{eff}})$.

In most of the experimental situations of interest it is well accepted that for driving frequencies less than the bubble resonance, thermal dissipation is the dominant damping mechanism; on the contrary, for frequencies greater than the bubble resonance, the scattering damping dominates [11–14] (for a review, see the book of Leighton, Chap. 4.4.2 [30]).

It is interesting to have a look at the form of each term of the dimensionless damping constant [10,14]:

$$\delta_{\text{v}}=\frac{4\mu_l\omega}{\rho_l R^2\omega_{\text{r}}^2}, \tag{10}$$

$$\delta_{\text{sc}}=\frac{R\omega^3}{c_l\omega_{\text{r}}^2}, \tag{11}$$

$$\delta_{\text{th}}=\frac{P_o}{\rho_l R^2\omega_{\text{r}}^2}\text{Im}[\tilde{F}(R,\omega)], \tag{12}$$

where $\tilde{F}(R,\omega)$ is a complex function that turns out to depend on the single variable $\eta=2R/l_{\text{t}}$, where $l_{\text{t}}=\sqrt{2D_g/\omega}$ is the gas thermal boundary layer thickness and D_g is the gas thermal diffusivity. The low frequency limit $\eta\to 0$ gives

$$\delta_{\text{th}}\to\frac{4R^2\omega}{3D_g}, \tag{13}$$

which is accurate within 5% and 10% for $\eta\lesssim 2.4$ and $\eta\lesssim 2.8$, respectively. The high frequency limit $\eta\to\infty$ gives

$$\delta_{\text{th}}\to\frac{3(\gamma-1)}{2R}\sqrt{\frac{2D_g}{\omega}}, \tag{14}$$

which in turn is accurate within 5% and 10% for $\eta\gtrsim 50$ and $\eta\gtrsim 25$, respectively. To give an idea of the relative value of the different damping terms, for a water/air mixture with $R\approx 10$ μm and $\omega/2\pi\approx 40$ kHz, we estimate $\delta_{\text{th}}\approx 1.6$, $\delta_{\text{v}}\approx 2.4\times 10^{-3}$, and $\delta_{\text{sc}}\approx 2.5\times 10^{-5}$. Thus, in the low frequency range, the thermal dissipation is indeed the dominant damping mechanism. Finally, in view of our experimental results, using Eqs. (13) and (14) in Eq. (9), such that $\delta\ll 1$, we find that for a water/air mixture the following scalings for the thermal contribution to the sound absorption are obtained:

$$\alpha_{\text{th}}\lambda\to\frac{4\pi\omega R^2}{3D_g} \tag{15}$$

for $\eta\to 0$ and

$$\alpha_{\text{th}}\lambda\to\frac{3\pi(\gamma-1)}{2}\sqrt{\frac{2D_g}{\omega R^2}} \tag{16}$$

for $\eta\to\infty$, where $c_{\text{eff}}=\lambda f$. We finally remark that these expressions are valid to leading order in δ.

II. EXPERIMENTAL SETUP

The experiment consists in measuring the propagation of acoustic pulses through aging foams. In all the experiments, shaving cream is used as a sample (Gillette regular [21]). This choice has been motivated in part by the number of experimental studies done on this kind of foam and in part by the stability and reproducibility of the samples [22–24].

Two different experimental setups are used depending on the explored acoustic frequencies. At low frequencies we only measure the sound velocity c. This is due to the fact that at low frequencies the acoustic absorption length $1/\alpha$ is of the order of 0.3–1 m [17], and we then need an experiment of these dimensions in order to measure it accurately. As we work with commercial shaving foams, we cannot produce these amounts of foam in a homogeneous way. At higher frequencies, as $1/\alpha$ becomes of the order of 1 cm or less, we are able to measure both c and α by probing the acoustic pressure as a function of the distance of propagation in a more reasonable volume of foam.

For all the experiments the average density of the foam $\langle\rho\rangle$ is controlled at the beginning of foam aging and after each measurement, at a given foam age. This is done by measuring the mass of foam contained in a known volume. The balance has a sensitivity of 0.01 g (Mettler Toledo PB602), so the final density sensitivity is $\approx\pm 2$ mg/cm^3. The foam temperature is maintained constant by controlling the ambient temperature at 21.5 ± 1 °C.

At low frequencies a 45-mm-diameter and 7-mm-thick piston is used as an acoustic source. Figure 1(a) shows a sketch of this setup. The frequency can be varied in the range 1 kHz–10 kHz. The experimental results presented here correspond to $f=5$ kHz. The piston is driven by an electromechanical vibration exciter (B&K 4810) and its response is followed by a piezoelectric accelerometer (B&K 4393). Fresh foam samples are injected in a 60-mm-interior-diameter and 90-mm-height cylindrical container. The container's wall is made of plexiglass and the vibrator is used as a base. With this setup, the foam is enclosed in the plexiglass tube (however, the sample is not sealed), and no humidity air saturation was found to be necessary. The incident acoustic pulse is obtained by means of exciting the vibrator with an amplitude modulated electric pulse, centered at a frequency f with N_c cycles. The reception is done by a piezoelectric pressure sensor with a 40 kHz resonant frequency (PCB 106B50), the sensitivity being 80.8 mV/kPa. As we measure both the piston response and the acoustic pressure, we can measure both the time of flight and the amplitude of the pressure signal. Thus, the distance between the piston surface and the pressure sensor is left fixed at $L=56$ mm, which ensures that measurements are done in the far field of the piston. The electric pulse is generated by an arbitrary function generator (Wavetek 395), and the number of cycles can be varied between a few cycles ($N_c=3$) to a semicontinuous pulse ($N_c\gtrsim 100$). Nevertheless, to avoid interferences due to reflections at the ends of the tube, all the pulses are chosen to

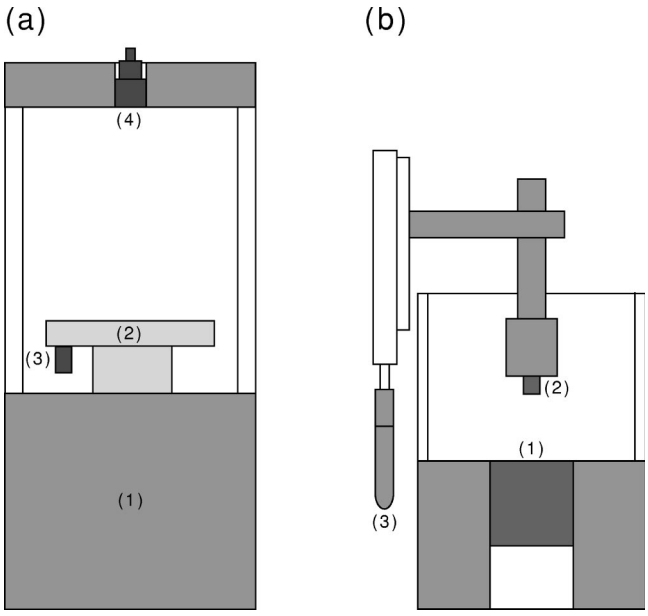

FIG. 1. Sketches of the experimental apparatus. (a) Low acoustic frequencies: (1) electromechanical vibration exciter, (2) piston, (3) piezoelectric accelerometer, and (4) pressure sensor. (b) High acoustic frequencies: (1) acoustic transducer, (2) pressure sensor, and (3) micrometer displacement controller.

be shorter than L (thus, in general, $N_c \lesssim 7$). This electric pulse is amplified by a power amplifier (B&K 2706) and the detected pressure signal is filtered and amplified by a low-noise preamplifier (Standford Research Systems 560). Typical gains vary between 10^3 and 10^4. The piston velocity and the amplified acoustic pressure signal are then measured by an oscilloscope (Lecroy 4374L) and transferred to a power PC via a general purpose interface bus board. The sound speed c is then obtained by measuring the time of flight τ_{fl} between the piston velocity and the pressure signal.

The second experimental setup is almost the same but the incident acoustic pulses are now generated by acoustic transducers. Figure 1(b) shows a sketch of this setup. To explore different frequencies, two different transducers are used for the pulse emission: a contact transducer is used at $f = 37$ kHz (Panametrics X1021) and an air coupled transducer at $f = 63$ and 84 kHz (ITC 9071). With this last transducer the acoustic impedance matching with the foam is much better. The fresh foam samples are injected in a 45-mm-diameter and 40-mm-height cylindrical container. The container's wall is plexiglass, while the base is polyvinyl chloride. The acoustic transducers are mounted concentrically on the base, with the active surface directed into the plexiglass cylinder. Thus, during an experiment, the acoustic transducer is in contact with the foam sample. In this case the reception is also done by a piezoelectric pressure sensor but with a 500 kHz resonant frequency (PCB 113A02). The sensor is followed by an in-line charge amplifier (PCB 402A11), the final sensitivity being 3.2 mV/kPa. The distance L between the acoustic transducer and the pressure sensor is controlled by a micrometer displacement controller, with a resolution of 20 μm (Micro-Controle M-UMR5.25). The electric signal generation and the pressure signal measurements are done in the same way as for the first setup. But in this case, the electric signal used to excite the acoustic transducers is amplified by a high speed power amplifier (NF Electronic Instruments 4005). Finally, the electric impulse and the amplified acoustic pressure are the signals that are measured by the oscilloscope and transferred to the power PC. To measure c and α, the distance L is varied by constant steps.

At high frequencies and for large distances of propagation, or large aging times, the acoustic pressures can be quite low, of the order of a few pascals. As the level of the electronic noise of the pressure sensor is of the order of 40 Pa, it is necessary to average the pressure signal for about 100 to 400 sweeps. Depending on the number of sweeps, this averaging process takes between 2 and 6 s, which is fast compared to the time evolution of the foam. Finally, within the second setup, only the upper surface of the foam sample is in contact with air. As the pressure sensor is immersed in the foam sample, this surface is always quite far from the probed volume, at least 20 mm farther. For the explored foam ages the evaporation of water is only seen to affect a thin layer on the surface of the sample, typically 1–2 mm thin. Thus, we do not need to saturate the air humidity because the probed volume is not affected by water evaporation. We verified this point by performing some measurements under humidity saturated atmosphere; no changes were observed.

An important point is the reproducibility of the experiments. We observe that our measurements are very sensitive to the foam production. As we use commercial shaving foams, the state of the initial foam varies from one sample to another. There are at least two important parameters: the foam average density $\langle \rho \rangle$ and the bubble size distribution $F(R,t)$, where t denotes the aging time. The foam density depends slightly on the foam tube history; it is mainly constant for the first 10–20 samples produced from the same tube (the foam then tends to become more liquid). For different tubes, we find that the density varies slightly. In general, the average foam density is measured to be $\langle \rho \rangle = 0.076 \pm 0.005$ g/cm^3, which corresponds to a gas volume fraction $\phi = 0.924 \pm 0.005$.

Once the density is controlled, the principal effect on the acoustic measurements is due to the bubble size distribution. We observe that for short evolution times, or low excitation frequencies, it is the mean bubble size $\langle R(t) \rangle$ that determines the foam acoustic properties. Nevertheless, as we increase the excitation frequency and tend to probe more effectively the ''details'' of the foam structure, the measurements become quite sensitive to the details of $F(R,t)$ and its evolution. It is clear that $F(R,t)$ is in part fixed by the interior geometry of the foam tube (size of pores through which the foam is forced, etc.), parameters that we do not control at all. Another parameter that is seen to affect $F(R,t)$ at the production of the foam is the velocity of the foam at the exit of the tube. In practice, this means that we have to produce the foam at a constant velocity, constant during its production and also between different sample productions.

To reduce then the possible errors due to the variations in $F(R,t)$ and $\langle \rho \rangle$ from one sample to another, we perform several measurements of α and c (between 5 and 20), keep-

ing unchanged the other experimental conditions. We then perform ensemble averages over α and c. This averaging procedure allows us to determine these quantities with relative errors smaller than 15% (in most cases 10%) and 5%, respectively.

III. EXPERIMENTAL RESULTS

A. Low frequency results

We start this section by presenting our experimental results at low frequency, namely, $f=5$ kHz and $N_c=5$. Figure 2 shows typical time series of the piston velocity v_p and the acoustic pressure p. The foam age is about 10 min and the initial time is given by the end of foam production. As the vibration exciter has a nearly flat frequency response around the excitation frequency, the piston velocity is seen to follow the electric pulse quite well. The acoustic pressure signal is also seen to follow the piston velocity, with the expected delay due to the pulse propagation. From this kind of data we define $p_{\max}$ and τ_{fl} as the maximum pressure amplitude of the acoustic pulse and the time between the maxima of the piston velocity and acoustic pressure pulse. Finally, the observed small second pulse in Fig. 2(b) is due to reflections at both ends of the tube, as its extra flight time is approximately double of the flight time of the first acoustic pulse.

We then present in Fig. 2(c) the time evolution of the ensemble-averaged sound velocity $c=L/\tau_{\mathrm{fl}}$, for ≈ 8 h of foam aging. To avoid confusions we note that we are dealing with the propagation of finite pulses and that there does not seems to be much pulse distortion, thus the measured velocity is the group velocity. As the system can be dispersive it should not be identified with the phase velocity. Measurements on five different foam samples were done. The error bars correspond to the standard deviations obtained. The ensemble-averaged density is $\langle\rho\rangle=0.076\pm0.005$ g/cm^3. For each sample the value of $\langle\rho\rangle$ is measured at the beginning of the foam aging. Within this setup the foam density does not vary during the first 2 h of foam aging. After 8 h of aging, a 5%–20% average decrease with respect to the initial value of $\langle\rho\rangle$ is measured. We observe that the exact value depends on the height at which the foam density is measured, the density change being higher near the top surface and smaller at the middle of the foam sample. In fact, for long times we observe the formation of a very thin layer of liquid on the vibration exciter surface, which confirms that the average density change is due to liquid drainage. The order of magnitude of the observed average density reduction is in agreement with previously published data [23].

We then observe a decreasing behavior of the sound velocity with time. At early times it has a value of 65 m/s and then decreases and tends to ≈ 50 m/s. The corresponding acoustic wavelength $\lambda=c/f$ varies from 1.3 cm to ≈ 1 cm with foam aging. This indeed corresponds to the large wavelength regime $\lambda \gg \langle R\rangle$. As expected from the discussions given in the Introduction, we measure a much lower effective sound speed compared to both sound speeds in the liquid and gas components of the mixture that composes the foam.

A very important experimental observation is that the foam softens with aging. This point has been clearly established for the shear elastic modulus of a coarsening foam [23,24]. However, the bulk elastic modulus of a foam does not seem to have been studied. Considering a foam as a viscoelastic solid, we can define the longitudinal sound speed as $c=\sqrt{(K+4\mu/3)/\langle\rho\rangle}$, where K and μ are the macroscopic bulk and shear elastic moduli, respectively [31]. Therefore, for fresh foams $c\approx 65$ m/s and then $K\approx 3.2\times10^5$ Pa, and after 2 h of coarsening $c\approx 53$ m/s, and K decreases to $\approx 2.1\times10^5$ Pa. We remark that we have used $K\gg\mu$, since a foam is usually considered as incompressible. In fact, we find that for fresh foams, K is ≈ 700 times larger than the reported values of μ [23,24]. It should be noticed that the frequencies of the shearing experiments reported in [23,24]

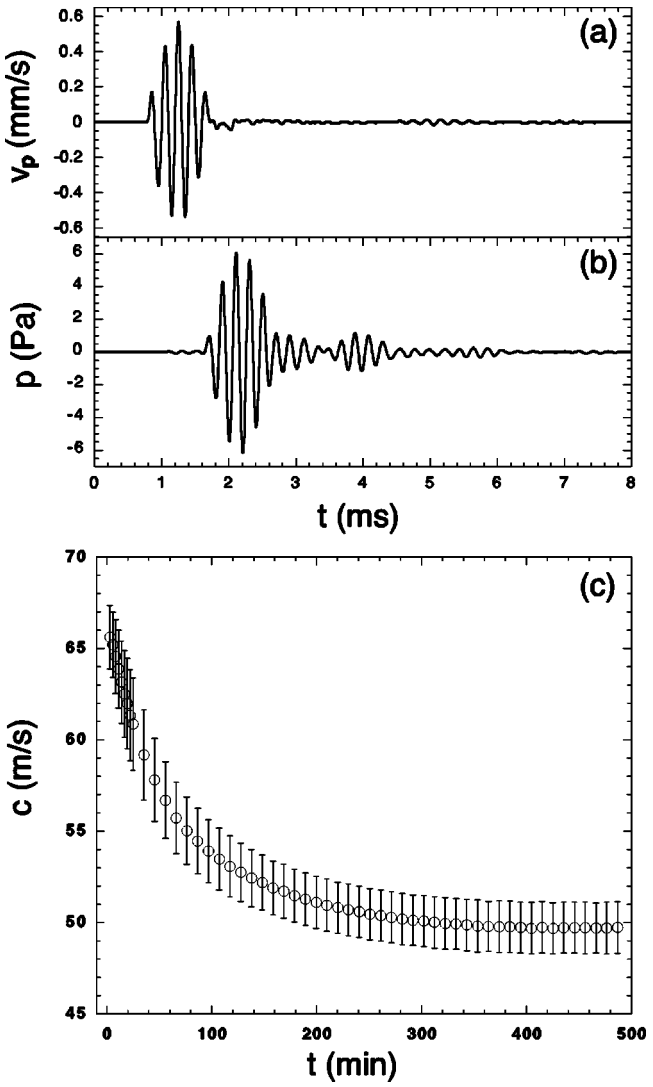

FIG. 2. Time series of piston velocity v_p (a) and acoustic pressure p (b), for $L=56$ mm, $f=5$ kHz, $N_c=5$, and $\langle\rho\rangle=0.074\pm0.002$ g/cm^3. Foam age is about 10 min. From this kind of data we define $p_{\max}$ and τ_{fl} as the maximum pressure amplitude of the acoustic pulse and the time of flight, which is measured between the maxima of the piston velocity and acoustic pressure pulse. (c) Time evolution of the ensemble-averaged sound velocity c for $f=5$ kHz. The ensemble-averaged density is $\langle\rho\rangle=0.076\pm0.005$ g/cm^3.

are very low, typically in the range $f=0.04$–3 Hz. Thus, the exact value of μ (to be compared with K) is expected to be different at $f=5$ kHz, but we do not expect it to change in order of magnitude.

Thus, as foam density does not vary significantly during the first few hours of foam aging, we can then conclude that the main mechanism responsible for the reduction of the sound speed with time is the increment of foam compressibility, or in other words, the softening of its elastic bulk modulus. Furthermore, we believe that the observed saturation of c is due to a competition between the increment of foam compressibility and the average density reduction in the foam's volume. In fact, measurements performed up to 17 h of foam aging show that c finally slightly increases with time, about 3% during the last 8 h. If the density reduction is the only mechanism for this small increment of c, we expect it to change by an amount of the order of 10%. Therefore, the observed long time behavior of c must be due to the competition between both effects.

The main results of the low frequency experiments are the following ones: (i) acoustic measurements allow us to probe the foam coarsening. (ii) As expected, the effective sound speed is found to be much lower than the sound speeds in both components of the foam. (iii) The sound speed reduction is due to the softening of the foam, i.e., the foam tends to be more compressible with aging time.

Nevertheless, for long times the liquid drainage is seen to affect the foam density profile, and thus sound propagation. Taking into account our observations on the evolution of $\langle\rho\rangle$, we then consider that acoustic measurements are of most utility during the first 4 h of foam coarsening. This means that we can use acoustic measurements for the determination of the bulk elastic modulus of a coarsening foam. For longer times, the main problem is the appearance of a density gradient in the system and a significant change of the average density; however, combined acoustic and density measurements can give important qualitative information about the foam properties and its aging.

B. High frequency results

We now present results concerning higher excitation frequencies, namely, $f=37$, 63, and 84 kHz. Considering the foam sound velocity to be of the order of 50 m/s, these frequencies correspond to wavelengths of the order of 1.3, 0.8, and 0.6 mm, respectively. We recall that our experimental setup allows us to measure both α and c in this frequency regime.

In Fig. 3 we present the time evolution of the pressure pulse maximum $p_{\max}$ and the flight time $\tau_{\rm fl}$ for $L=15$ mm, $f=37$ kHz, $N_c=7$, and $\langle\rho\rangle=0.078\pm0.002$ g/cm^3. We note that the flight time $\tau_{\rm fl}$ is now defined as the time difference between the maxima of the electric input and the acoustic pulse. We observe that as the foam coarsens the transmitted acoustic signal becomes smaller. After 90 min, the acoustic amplitude $p_{\max}$ decreases approximately by a factor of 50. Thus, at high frequencies and as the mean bubble size increases with time, the acoustic absorption in the foam increases in a significant way. Also, after

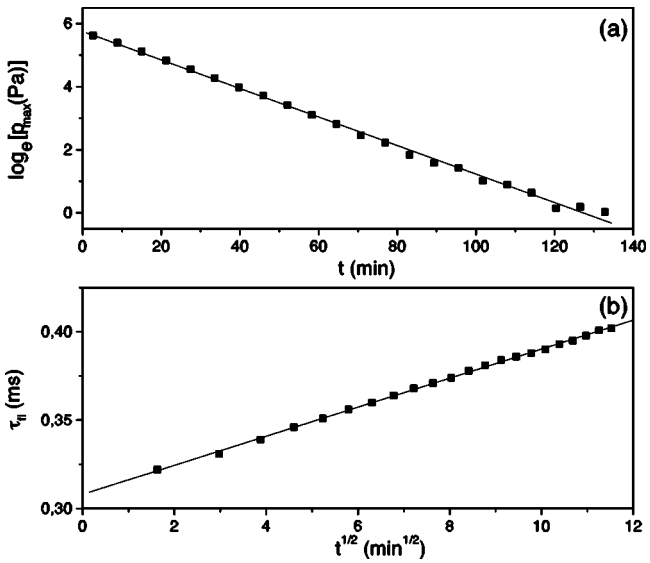

FIG. 3. (a) In log$_e$-linear scale, time evolution of $p_{\max}$ for $L=15$ mm, $f=37$ kHz, $N_c=7$, and $\langle\rho\rangle=0.078\pm0.002$ g/cm^3. (b) $\tau_{\rm fl}$ vs $t^{1/2}$. Continuous lines show the fits $p_{max}=p_o e^{-t/\tau}$ and $\tau_{\rm fl}=a+bt^{1/2}$, with $p_o=314\pm3$ Pa, $\tau=22.1\pm0.3$ min, $a=0.308\pm0.001$ ms, and $b=8.2\pm0.1$ μs/min$^{1/2}$.

this time, the flight time $\tau_{\rm fl}$ slightly increases. Thus, as we already observed at low frequencies, as the foam coarsens, sound velocity decreases. Figure 3(a) shows that $p_{\max}$ decreases exponentially with time, with a characteristic decay time τ of the order of 22 min. We note that this decay time depends on L, and we roughly find $\tau\propto 1/L$. At this propagation distance, $L=15$ mm, after 120 min the acoustic signal decreases to ≈ 1 Pa. This value corresponds to the resolution of our acquisition system (sensor sensitivity + averaging process + oscilloscope resolution). On the other hand, Fig. 3(b) shows that $\tau_{\rm fl}$ evolves according to the law $a+bt^{1/2}$, with $a=0.308\pm0.001$ ms and $b=8.2\pm0.1$ μs/min$^{1/2}$. We remark that these ''nice'' behaviors of $p_{\max}$ and $\tau_{\rm fl}$ with aging time t are not observed at low frequencies.

An important feature is the dependence of $p_{\max}$ and $\tau_{\rm fl}$ on L. As the foam evolves with time, we must make fast measurements for different values of L. The term ''fast'' means that the measurement should take a time much smaller than the typical decay times. This is done by moving the pressure sensor manually with the micrometer displacement controller and measuring $p_{\max}$ and $\tau_{\rm fl}$. The motion is in the direction of the acoustic transducer, so we decrease L by constant steps. A typical run for several L's takes about 1 min, which is indeed short compared to the decay times. Figure 4(a) shows that $p_{\max}$ also decreases exponentially with L (for a ''fixed'' evolution time). The data were taken 30 min after the foam production. The continuous line shows an exponential fit of the form $p_{\max}=p_o e^{-\alpha L}$, with $p_o=1.07\pm0.01$ kPa and $\alpha=160\pm3$ m^{-1}. Now, we define $\Delta L=L-L_1$ and $\Delta\tau_{\rm fl}=\tau_{\rm fl}-\tau_{\rm fl1}$, where L_1 and $\tau_{\rm fl1}$ are the shortest measured distance of propagation and flight time. Figure 4(b) then presents ΔL as a function of $\Delta\tau_{\rm fl}$, and the slope of this curve gives a direct measurement of sound velocity; in this case $c=55.1$

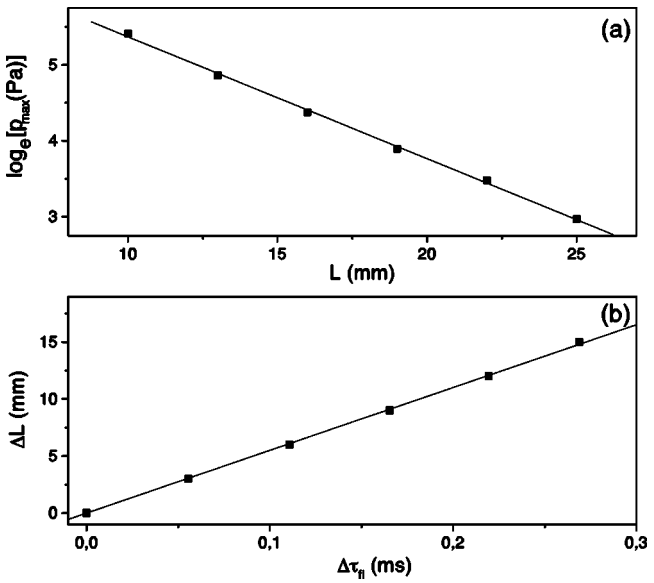

FIG. 4. (a) In $\log_e$-linear scale, $p_{\max}$ versus L. (b) ΔL versus $\Delta\tau_{\rm fl}$. The continuous lines show the fits $p_{max}=p_o e^{-\alpha L}$ and $\Delta L = c\Delta\tau_{\rm fl}$, with $p_o=1.07\pm0.01$ kPa, $\alpha=160\pm3$ 1/m, and $c=55.1\pm0.3$ m/s. The measurement was made 30 min after the foam production. $f=37$ kHz, $N_c=7$, and $\langle\rho\rangle=0.080\pm0.002$ g/cm^3.

±0.3 m/s. We remark that this method avoids the effects of the thin liquid layer between the transducer and the foam formed by drainage [32].

Considering our experimental results we observe, as expected, that the acoustic pressure has the following form:

$$p(x,t)\propto p_{\max}(x,t)e^{i[\omega t-k(t)x]}, \tag{17}$$

$$p_{\max}(x,t)\propto e^{-\alpha(t)x}, \tag{18}$$

where $k(t)=\omega/c(t)$ is the wave number, $c(t)$ is the sound velocity, and $\alpha(t)$ is the absorption coefficient [the $\alpha(t)$ and $c(t)$ notation indicates the effect of foam coarsening]. These are the basic acoustic quantities that we can measure. We note that in our problem there are clearly two different time scales, one associated with the foam evolution and the other with the sound frequency, such that $\tau\gg1/f$. There are also three length scales, given by λ, $1/\alpha$, and $\langle R\rangle$, which in general are well separated, i.e., $1/\alpha>\lambda\gg\langle R\rangle$. However, as will be shown for high frequencies and large foam ages, the absorption length can be comparable to the acoustic wavelength, $\lambda\sim1/\alpha$ (see below).

The evolution in time of $\alpha\lambda$ and c for different frequencies is displayed in Fig. 5. For comparison, we also show in Fig. 5(b) the values of c obtained at $f=5$ kHz. At high frequencies, each point corresponds to an ensemble average of at least seven independent experimental runs.

We observe that $\alpha\lambda$ increases with time for all f. Also, for a fixed foam age, $\alpha\lambda$ increases with f. Thus, we can conclude that as we probe the smaller scales of the foam structure (by increasing $\langle R\rangle$ or decreasing λ) the sound is more effectively attenuated. We observe that the fluctuations of $\alpha\lambda$ increase with both f and the foam aging time (see the size of the error bars). This reflects the sensitivity of the acoustic absorption measurements to the details of the foam disorder. We also observe that as foam coarsens, the two length scales $1/\alpha$ and λ become comparable.

Another interesting feature is that after an initial transition time of ≈20 min, $\alpha\lambda$ seems to follow a linear dependence on t. We present then in Fig. 5(a) the corresponding linear fits $\alpha\lambda=a+bt$, which are done for $t>20$ min. These linear evolution laws fit quite well the ensemble-averaged values of $\alpha\lambda$. Recalling the parabolic law Eq. (1), we conclude that the time dependence of the quantity $\alpha\lambda$ is given by the evolution of the square of the dominant length scale in the foam, the mean bubble radius, i.e., $\alpha(t)\lambda(t)\propto\langle R(t)\rangle^2$.

Concerning sound velocity, we observe that at high frequencies c also decreases with time; it has an initial value of the order of 63 m/s and it decreases to ≈45 m/s after 4 h of aging. As the density does not change significantly on the evolution time scale, we confirm our previous result that the

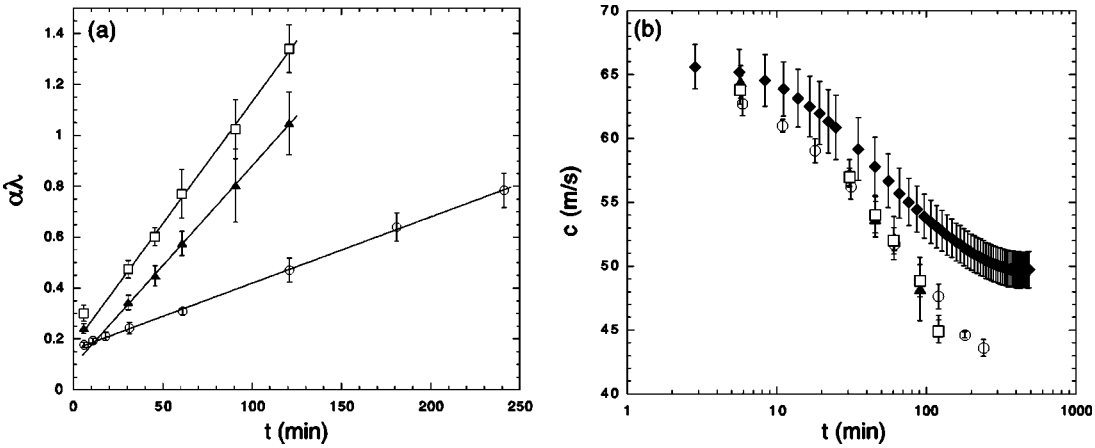

FIG. 5. (a) Time evolution of $\alpha\lambda$ for $f=37$ (○), 63 (▲), and 84 (□) kHz. The continuous lines correspond to linear fits $\alpha\lambda=a+bt$ for $t>20$ min. The parameters are $a=0.159$, 0.097, and 0.175, $b=2.61\times10^{-3}$, 7.84×10^{-3}, and 9.58×10^{-3} min^{-1}, respectively. The linear regression coefficients are $R_c=0.9996$, 0.9998, and 0.9992, respectively. (b) Time evolution of c, in linear-$\log_{10}$ scale, for $f=5$ (◆), 37 (○), 63 (▲), and 84 (□) kHz. The ensemble-averaged density is $\langle\rho\rangle=0.076\pm0.005$ g/cm^3.

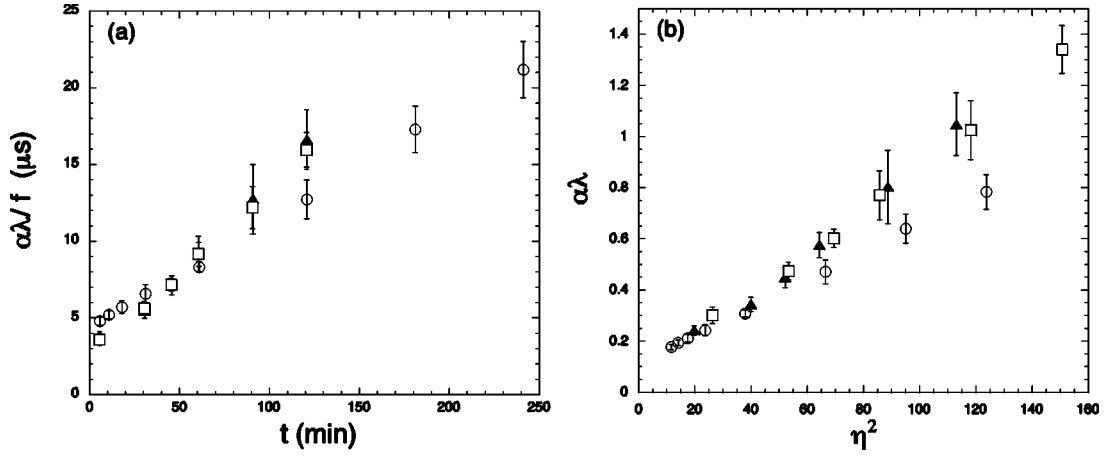

FIG. 6. (a) Time evolution of the scaled quantity $\alpha\lambda/f$. (b) $\alpha\lambda$ versus $\langle\eta\rangle^2$, where $\langle\eta\rangle=2\langle R\rangle/l_t$; $f=37$ (○), 63 (▲), and 84 (□) kHz, and $l_t=6.6$, 5.0, and 4.4 μm, respectively.

foam softens as it coarsens. Concerning the frequency dependence we note that for short times we do not observe any velocity dispersion. Nevertheless, as time evolves a clear velocity dispersion appears; after 2 h of aging, the lowest frequency value is clearly higher than the highest frequency value, by approximately a factor 20%, and c thus becomes a decreasing function of f. We believe that the only possible explanation for this time-dependent velocity dispersion is the existence of a characteristic time scale that depends on the mean bubble radius $\langle R(t)\rangle$. A natural choice seems to be the inverse of the bubble resonant frequency. In fact, in the limit $\phi\ll 1$, sound velocity dispersion is observed as the resonant frequency is approached [8,10], and for $\omega\lesssim\omega_r$, c decreases with f. We note that this velocity dispersion is also predicted by the dispersion relation (6). Nevertheless, the definition of a resonant frequency in a concentrated foam does not seem clear, and we do not have the analogous expressions to Eqs. (5) and (6).

From the velocity data of Fig. 5(b), we can estimate the evolution of the ratio $\lambda/\langle R\rangle$ for all the explored frequencies. To obtain $\langle R\rangle$ we use Eq. (1) and we roughly estimate $A=5.07$ μm^2/min, $t_o\approx 20$ min, and $\langle R_o\rangle\approx 14$ μm, using the visual observations reported in Ref. [24]. We obtain that $\lambda/\langle R\rangle$ decreases asymptotically as a power law of t, which is due to the parabolic evolution of $\langle R\rangle$ and the very small dependence of λ on t. Depending on both the foam age and the excitation frequency, this quantity decreases from ≈ 1500 to 20. Thus, due to the explored frequency range and the foam coarsening, we see that our experiments explore both regimes $\lambda\gg\langle R\rangle$ and $\lambda\approx 20\langle R\rangle$.

To conclude the presentation of our experimental results, we plot in Fig. 6(a) the time evolution of $\alpha\lambda/f$, for all f together. We notice that this scaling works pretty well, specially at the shorter aging times, let us say for $t\lesssim 90$ min.

Thus, the main results of the high frequency experiments are the following.

(i) Sound attenuation varies significantly with both foam age and sound frequency. As we probe the smaller scales of the foam structure, by increasing $\langle R\rangle$ or by decreasing λ, the sound is more effectively attenuated. The sound attenuation fluctuations are also seen to increase with time and frequency.

(ii) For all the explored frequencies the sound velocity decreases with foam age. Thus, the foam becomes more compressible as it coarsens. Velocity dispersion is observed for long evolution times. After 2 h of foam coarsening c has clearly become a decreasing function of f.

(iii) The attenuation per wavelength $\alpha\lambda$ is seen to be a linear function of foam age, i.e., $\alpha\lambda\propto t$. Recalling the parabolic law for the evolution of $\langle R(t)\rangle$, we can then state that this quantity scales as $\alpha\lambda\propto\langle R\rangle^2$. In addition, for short times, $\alpha\lambda$ is found to scale linearly with both foam age and frequency, so that $\alpha\lambda\propto tf\propto\langle R\rangle^2 f$.

IV. DISCUSSION AND CONCLUSIONS

A. Sound attenuation

Our measurements show that the acoustic attenuation is very high compared to the attenuation in both components of the foam. We can qualitatively understand this fact by following an argument given by Landau and Lifshitz [33]. Let us suppose that we have a gas bounded by a well defined surface, which has both high thermal conductivity and high rigidity compared to the gas, and consider that a sound wave in the gas undergoes a reflection on the wall's surface. In the sound wave, the temperature oscillates periodically about its mean value. Thus, near the rigid and highly conductive wall, there is a periodically fluctuating temperature difference between the gas and the wall. But at the wall itself, the temperatures of the wall and the fluid must be the same. This generates a large temperature gradient in a thin boundary layer of the gas, where energy is dissipated by thermal conduction. The same kind of argument shows that the gas viscosity also leads to a strong absorption of energy, because the velocity gradient is large at the boundary. We recall that in the bulk of a homogeneous fluid, sound attenuation is due to the same physical mechanisms, but the temperature and velocity gradients are generated by the wave itself, such that they are of order T_{ac}/λ and v_{ac}/λ, respectively [33]. Here,

T_{ac} and v_{ac} are the amplitude of the acoustic temperature and velocity fluctuations. In general, these gradients are small compared to the gradients formed in a boundary layer. In fact, it is well known that the ratio of the power losses at the surface to the power losses in the gas volume is of order λ/l, where l is the molecular mean free path in the gas (see Chapter 6.4 in Ref. [34]). This can be easily shown by estimating the thermal power losses on the wall, Π^t_{wall}, and the thermal power losses in the volume, Π^t_{vol}, as

$$\Pi^t_{wall} \propto (T_{ac}/l_t)^2, \quad \Pi^t_{vol} \propto (T_{ac}/\lambda)^2, \tag{19}$$

where $l_t = \sqrt{2D_g/\omega}$ is the thermal boundary layer. Thus,

$$\frac{\Pi^t_{wall}}{\Pi^t_{vol}} \propto \left(\frac{\lambda}{l_t}\right)^2 \propto \frac{\lambda}{l}, \tag{20}$$

where in the last expression we have used $D_g \approx c_g l$, l being the molecular mean free path in the gas and c_g the gas sound speed. In a gas, $\nu \approx c_g l/\sqrt{\gamma}$, and the same result is obtained for the ratio of the viscous power losses. The fact that the surface power losses dominate the volume power losses explains why systems of high porosity and with high contrasts of both thermal and acoustic properties, such as foams, are good acoustic attenuators.

As discussed in Sec. I B, there are several damping mechanisms of an acoustic wave in a bubbly liquid, namely, the liquid viscosity, the gas thermal conductivity, and the sound scattering. In principle, from both the frequency and the bubble size dependence of $\alpha\lambda$, we should be able to identify which of these mechanisms is dominant. In our experiments, the bubble sizes vary with time due to gas diffusion, according to an evolution law of the form $\langle R\rangle^2 \propto t$. As we measure a linear dependence of $\alpha\lambda$ with time, we conclude that $\alpha\lambda \propto \langle R\rangle^2$. This scaling alone is a strong restriction to the possible damping mechanisms. On the other hand, we observe that the quantity $\alpha\lambda$ scales like f for early foam ages, approximately for $t \lesssim 90$ min.

If we consider the scattering contribution given by Eq. (12), we should expect a dependence of the form $\alpha_{sc}\lambda \propto R\omega^3/\omega_r^2$. This corresponds to Rayleigh scattering, $\alpha \propto \omega^4$, valid in the large wavelength limit $\lambda \gg R$. As discussed before, in the case of concentrated foams, it is clear that ω_r cannot be given by Eq. (5), and the question of a proper definition of the bubble resonance in a concentrated foam does not seems to be clear. As the density is greatly reduced compared to a dilute bubbly liquid, we do expect the resonance to be shifted to higher frequencies. In any case, in the large wavelength regime, a Rayleigh scaling $\alpha_{sc}\lambda \propto \omega^3$ is expected. Thus, from our experimental results we can conclude that the scattering damping is not important to leading order.

An important point that has not been discussed is the viscous attenuation caused by the translational motion of the bubbles. In fact, the van Wijngaarden–Papanicolaou model considers the viscous attenuation due to the radial motion of the bubbles. But it has been argued that in the case of bubbly liquids, for frequencies much smaller that the bubble resonant frequency, the effects of viscosity on the translational motion would dominate the effects caused by the radial oscillations [3,35]. Nevertheless, as discussed in the Introduction, it has been well established for bubbly liquids that the thermal damping dominates for $\omega \ll \omega_r$ and $\phi \ll 1$ [10], such that even if the translational viscous drag dominates the radial viscous damping, it does not seem to be important. In general, the relative importance of the different damping mechanisms depends on the material constants of the system. For example, Urick compares experimental results of sound attenuation in dilute kaolin and sand suspensions with a viscous-drag calculation of α_v [36]. He finds a good agreement with theory and he concludes that the viscous drag between the fluid and the particles is the dominant damping mechanism. On the other hand, Allegra and Hawley compare viscous drag and thermal attenuations in an emulsion of 20% toluene in water and find that the thermal damping is dominant [37].

We must note that the asymptotic viscous-drag expressions of $\alpha_v\lambda$ [36,37] take forms similar to those given by Eqs. (15) and (16) for the thermal damping mechanism, such that

$$\alpha_v\lambda \propto \frac{\omega R^2}{\nu_l} \tag{21}$$

for $R/l_v \ll 1$, with $l_v = \sqrt{2\nu_l/\omega}$, and

$$\alpha_v\lambda \propto \sqrt{\frac{\nu_l}{\omega R^2}} \tag{22}$$

for $R/l_v \gg 1$. Thus, compared to our results, both low frequency expressions (15) and (21) give the correct scalings on R and ω. As the foam is concentrated, it seems quite unlikely to us that the sound wave could generate a relative motion between the bubbles and the thin liquid films. To clear up this point, we estimate the viscous boundary layer for $f = 37$, 63, and 84 kHz to be $l_v \approx 2.9$, 2.3, and 1.9 μm, respectively, where we approximate $\nu_l \approx 10^{-6}$ m^2/s, as for water. As the liquid channel thickness h in our foams is ≈ 1 μm or less, we conclude that bubbles are strongly coupled by viscous forces. The viscous forces are then so high, that no relative motion between the bubbles and the liquid is possible. However, if the frequency is increased enough, such that l_v decreases well below h, we can expect the viscous-drag attenuation to become important. We finally conclude that the main contribution to the sound attenuation is given by thermal dissipation.

We can indeed go a step further by comparing quantitatively our results with the theoretical predictions for the thermal attenuation. To do so, we plot in Fig. 6(b) the experimental attenuation per wavelength versus $\langle\eta\rangle^2$, where $\langle\eta\rangle = 2\langle R\rangle/l_t$. The gas is a mixture of isobutane and propane, we then have $D_g \approx 5\times 10^{-6}$ m^2/s at $T \approx 21.5\,^\circ$C [38]. Once again, $\langle R\rangle$ is estimated by the parabolic law (1). As the bubble size distribution is quite large, we recall that $\langle\eta\rangle$ is an average value. For $f = 37$ kHz and at the beginning of foam coarsening, $\langle\eta\rangle \approx 3$; for long aging times and higher frequencies, $\langle\eta\rangle \approx 12$. Thus the bubble diameter is, in general, larger

than the thermal boundary layer. We observe that for the smaller values of $\langle \eta \rangle^2$, the data collapse on a single curve. This collapse also corresponds to the smaller values of $\alpha\lambda$. For higher values of $\langle \eta \rangle^2$, $\alpha\lambda$ seems to increase with *f*. A possible explanation is that when we increase the frequency, the scattering contribution of the larger bubbles to the sound attenuation becomes important. The crossover between the different behaviors is obtained for $\langle \eta \rangle^2 \approx 40$.

We note that from Eq. (16) we expect $\alpha\lambda \propto 1/\langle \eta \rangle$ for $\langle \eta \rangle \gg 1$. This means that for a large enough frequency, $\alpha\lambda$ should decrease with *t*, which is not observed experimentally. We think that this is in part due to the large polydispersity of the bubble size distribution. In fact, we expect a maximum attenuation per wavelength for $\eta \sim 1$, which can be interpreted as a thermal resonance condition $l_t \sim R$. Thus, at fixed frequency, the bubbles that satisfy this thermal resonance condition are those that attenuate most effectively the incident sound wave. Due to foam coarsening, the bubble size distribution becomes larger with time. However, the smallest bubbles are continuously shrinking before disappearing during the coarsening process. Thus, there always exist bubbles that satisfy the resonance condition even at high frequency. On the other side, for the larger bubbles, the scattering contribution to the sound attenuation becomes important. These two mechanisms lead to an increase of $\alpha\lambda$ with time.

B. Effective sound velocity

Our first observation is that the value of the sound velocity is much smaller that the velocities of both components of the foam, which is expected from the high contrast of acoustic properties between the components of the foam. As it will become clear after this discussion, the most important experimental observations are the following: (i) The sound speed evolves as the foam coarsens. (ii) The initial value of *c* is markedly higher than that estimated with Wood's formula (3). (iii) Velocity dispersion is observed for long times; after 2 h of foam coarsening, *c* is clearly a decreasing function of *f*. These results show that the sound speed depends on the foam structure in a nontrivial way, and we will now discuss them in more detail.

We can indeed try to estimate the sound velocity by means of the effective-medium approximation. We use Wood's formula, given by Eq. (3). The foam average density is $\langle \rho \rangle \approx 0.076$ g/cm^3, and we can consider the average compressibility to be $\langle \chi \rangle \approx \phi \chi_g$, where $\phi \approx 0.924$ is the average gas volume fraction and $\chi_g \approx 1/\gamma P_o$ is the adiabatic compressibility of the gas. Here, P_o is the atmospheric pressure and γ is the ratio of specific heats. As the gas is a mixture of isobutane and propane, we approximate $\gamma \approx 1.1$ for $T \approx 21.5\,^\circ$C [38]. Thus, $\chi_g \approx 8.8 \times 10^{-6}$ Pa^{-1}, and we find $c_{\text{eff}} \approx 40$ m/s, which is of the order of magnitude of the measured values. For fresh foams the sound velocity has nevertheless a value of 65 m/s, which is $\approx 60\%$ higher than the estimated value. This seems to be contradictory, because at the beginning of the foam evolution the condition $\lambda \gg \langle R \rangle$ is better satisfied than for large foam ages, so we would expect the effective-medium estimation to work better at short foam ages. The difference between the predicted and the measured values of *c* has already been noted by Gol'dfarb *et al.* [20], and it seems that there is a systematic deviation in some of the measured values compared to the adiabatic approximation given by Eq. (3). Nevertheless, some experimental results presented in Ref. [20] agree with Eq. (3). This confusing result was already pointed out in the introduction of this paper. We note that Gol'dfarb *et al.* did not take into account the foam coarsening. No attention at all was drawn to the age of the foam when the measurements were done. Our measurements indicate that the value $c \approx 40$ m/s can be observed if the foam coarsens for long enough time. However, there is an important difference between the estimated and the measured values of *c* for fresh foams.

The estimation given by Wood's formula must be considered as a leading order approximation. In fact, we have found that the effective sound velocity evolves with time, and this aspect is not considered at all in this effective-medium approach. We know that for the first hours of foam coarsening the average density $\langle \rho \rangle$ does not vary significantly with time. We must then consider the dependence of the compressibility on the foam structure. In particular, for short foam ages, we expect that the effective compressibility should be lower, roughly by a factor 2.5 with respect to $\phi/\gamma P_o$.

It is well known that the presence of surfactant molecules gives elastic properties to liquid films [39,40]. This elasticity is caused by the redistribution of the surfactants between the free surface and the bulk of the liquid during a deformation process. When the deformations are slow, this elasticity is called Gibbs elasticity. Thus, during a slow deformation, the surfactant molecules have time to diffuse out to the surface. There is then a thermodynamic equilibrium between the surface and the bulk surfactant concentrations. On the contrary, if the deformation is fast, the elasticity is called Marangoni elasticity, and in this case the surfactant molecules do not have time to migrate from the bulk to the free surface. In this case, the deformation changes the film's surface but the number of surfactant molecules at the surface stays constant. When the liquid film is stretched, the surfactant surface concentration is then reduced and the surface tension increases. It is the extra surface tension that tends to reduce the surface deformation.

The terms ''slow'' and ''fast'' must be compared to a diffusion time scale. In fact, it is the time $\tau_D = h^2/D_{\text{ch}}$ that characterizes the diffusive motion of the surfactant molecules (here *h* is the liquid film thickness and D_{ch} is a chemical diffusion constant). Typically, for 1-μm-thick films, τ_D is of the order of 0.01 s [40]. However, due to contaminations, τ_D can increase up to 1 s [39]. It is then clear that for the explored acoustic frequencies, it is the Marangoni elasticity that could be important. For small surfactant concentrations, the Gibbs and Marangoni elastic constants are of the same order, $E_{\text{G}} \approx E_{\text{M}} \approx 80$ mN/m [40]. For large concentrations, the Marangoni elasticity dominates, the value of E_{M} being smaller than in the small concentration limit.

We can then consider that the foam liquid matrix has elastic properties. The problem of sound propagation through a liquid-elastic matrix with gas inclusions resembles very much that of a porous fluid-filled solid media (in our case the fluid is the gas and the porous ''solid'' medium is the liquid-

elastic skeleton). In fact, sound propagation through these kind of heterogeneous systems has been widely studied. The semiphenomenological Biot theory is considered as the most general effective-medium theory for two-component systems and it has been shown to have a tremendous predictive power [41]. To our knowledge, this is the only effective-medium theory that considers explicitly the existence of a skeleton elasticity, and it is therefore interesting to see under which circumstances we can apply this theory to our foam samples. In the Biot theory there are four basic assumptions [41]: (i) the system can be described by two displacement fields, (ii) there is no force due to relative displacements of the centers of mass of the two constituents, (iii) the fluid (in our case the gas) neither creates nor reacts to shear forces, (iv) sound attenuation is solely due to viscous damping created by the relative motion of both constituents. To apply this theory to our foams, the main problems are given by assumptions (ii) and (iv). In fact, assumption (ii) presumes that the fluid is interconnected throughout the sample, which is not the case in a foam. On the other hand, assumption (iv) neglects the possibility of thermal damping, which we know is dominant for the high frequencies explored by our experiments. However, it is easy to show that point (ii) can be completely relaxed if both constituents are described by the same displacement field, such that there is no relative motion between the gas and the liquid; as it has already been shown, this is the case for our foam samples because bubbles are highly coupled by viscous forces. This has another consequence, which is the elimination of dissipative terms in Biot theory, since the only damping source is given by velocity differences at the boundaries of both constituents.

Thus, the main problem is that Biot theory does not consider thermal attenuation. However, we note that in the low frequency experiments $p_{\max}$ decreases very slowly during the explored aging times, by approximately a factor of 1.6 after 8 h of coarsening. This has to be compared to the reduction of $p_{\max}$ by a factor of 50 observed after only 2 h of coarsening for $f=37$ kHz. If we assume that at low frequencies, thermal damping dominates the acoustic attenuation, then for $f=5$ kHz, $\alpha\lambda\propto\langle R\rangle^2\omega$ is of order 0.03, 0.07, and 0.1 for aging times of 20 min, 2 h and 4 h, respectively. Thus, our low frequency experiments can be considered as almost nondissipative. We can then apply the low frequency results of the Biot theory. In this limit, both constituents are described by the same displacement field and two nondissipative propagating modes are predicted [41], a transverse mode and a longitudinal one, with speeds given by

$$c_{\mathrm{t}}^2=\frac{N}{\langle\rho\rangle},\quad c_{\mathrm{l}}^2=\frac{H}{\langle\rho\rangle} \tag{23}$$

with

$$H=\frac{K_s+[\phi(K_s/K_f)-(1+\phi)]K_b}{1-\phi-K_b/K_s+\phi(K_s/K_f)}+\frac{4}{3}N, \tag{24}$$

where ϕ is the fluid volume fraction. K_s and K_f are the bulk elastic moduli of the solid and the fluid as if they were homogeneous and isotropic. Thus, in the case of a foam, $K_s\to 1/\chi_l$ and $K_f\to 1/\chi_g$, and ϕ is the gas volume fraction. K_b and N are the bulk and shear elastic moduli of the skeletal frame (liquid-elastic matrix). In general, they are independent of the fluid in the pores [41]. N can be then identified as the shear modulus of the foam, previously noted by μ, but for a foam $\mu\propto\sigma/\langle R\rangle$ [23,24] and the surface tension σ depends on the gas. On the other hand, the first term of H can be then identified as the elastic bulk modulus, which we denoted by K in Sec. III A. For a foam $K\gg\mu$, and we can then consider that the first term of the right-hand side of Eq. (24) is dominant. The form of this term is not obvious, but we can show that in the limit of a very weak skeleton, such that $K_b/K_s\to 0$ and $K_b/K_f\to 0$, Eq. (24) then takes the form

$$H\approx\frac{1}{\phi\chi_g+(1-\phi)\chi_l}, \tag{25}$$

and the longitudinal sound velocity c_1 takes the form of Wood's formula (2). In the case of a foam, where the elastic properties of the liquid films can be important, we have

$$H\approx\frac{1}{\phi\chi_g}(1+\phi\chi_g K_b), \tag{26}$$

where we have neglected terms of order χ_l/χ_g. Thus, the skeleton elastic modulus K_b increases the foam's effective bulk modulus, and thus the effective sound speed.

We now proceed to estimate K_b. It is known that pure liquid films (without surfactants) can propagate in both antisymmetrical and symmetrical wave modes [40]. However, the symmetrical mode is more difficult to observe because it involves viscous motion of the liquid from the nodes to the antinodes. In a liquid film with surfactant molecules, the variation of thickness is coupled to the variation of the surface density of the surfactant molecules. The corresponding waves propagate at a velocity $v_{\mathrm{M}}=\sqrt{2E_{\mathrm{M}}/\rho_l h}$ [40], where h is the film thickness. We can therefore define the liquid film elastic modulus as $K_b\approx 2E_{\mathrm{M}}/h$.

The final step is to relate h to the mean bubble radius $\langle R(t)\rangle$. As the total foam surface decreases with time and the liquid content is constant, h should increase with time. In addition, as the foam structure is dominated by a single length scale, a linear relation $h\propto\langle R(t)\rangle$ is expected. We then estimate an average value of h by assuming that each bubble is surrounded by a liquid film of thickness $h/2$ (thickness per bubble). The gas volume fraction is then

$$\phi\approx\frac{\langle R(t)\rangle^3}{\langle R(t)+h(t)/2\rangle^3}. \tag{27}$$

Thus, for $\phi\approx 0.924$, $\langle h(t)\rangle=B\langle R(t)\rangle$, with $B\approx 5.34\times 10^{-2}$. The effective skeleton elastic modulus is therefore

$$K_b\approx\frac{2E_{\mathrm{M}}}{B\langle R(t)\rangle}. \tag{28}$$

We then find that the foam's effective bulk modulus, given by Eq. (26), evolves with time, which explains the

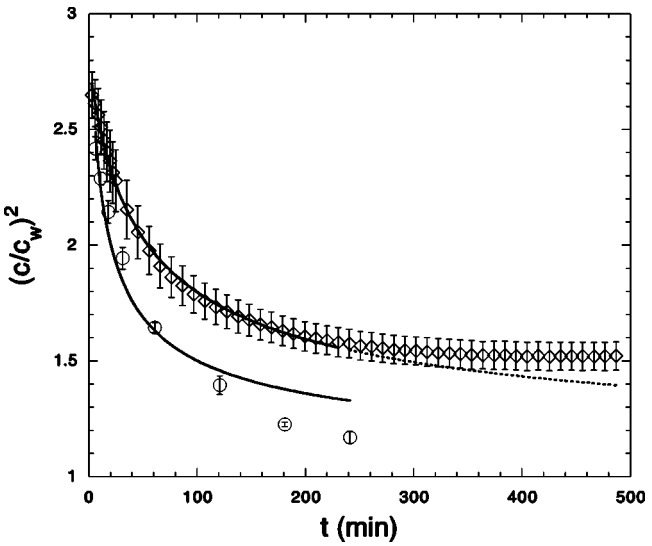

FIG. 7. Time evolution of $(c/c_{\mathrm{w}})^2$ for $f=5$ ($\diamond$) and 37 ($\bigcirc$) kHz. The continuous lines correspond to fits of the form $[c(t)/c_{\mathrm{w}}]^2=1+a/\sqrt{1+b(t-t_o)}$ for $t<240$ min (see Table I for the values of a and b). The dashed line shows the extrapolation of the fit for $f=5$ kHz.

time dependence of the measured sound velocity. In fact, using Eqs. (23), (26), and (28), we find that the longitudinal sound speed takes the form

$$\left(\frac{c_{\mathrm{l}}(t)}{c_{\mathrm{w}}}\right)^2=1+\frac{a}{\sqrt{1+b(t-t_o)}} \tag{29}$$

with $c_{\mathrm{w}}=\sqrt{\gamma P_o/\phi\langle\rho\rangle}\approx 40$ m/s, which is Wood's value of the effective sound speed, and

$$a=\frac{2\phi E_{\mathrm{M}}}{B\gamma P_o\langle R_o\rangle}, \tag{30}$$

$$b=\frac{A}{\langle R_o\rangle^2}. \tag{31}$$

As before, $A\approx 5.07$ μm^2/min and $\langle R_o\rangle\approx 14$ μm, thus $b\approx 0.026$ min^{-1}.

We then present in Fig. 7 the time evolution of the experimental values of $(c/c_{\mathrm{w}})^2$ for $f=5$ and 37 kHz. This quantity represents the foam's elastic bulk modulus, normalized to $\gamma P_o/\phi$. As discussed before, for early times of coarsening, this bulk modulus is a factor 2.5 higher than $\gamma P_o/\phi$. In the frame of the Biot theory we can understand this fact by the importance of the liquid matrix intrinsic elasticity, which turns out to be of the same order as $\gamma P_o/\phi$. The continuous lines are fits of Eq. (29) for $t<240$ min, where both a and b are adjustable parameters. We observe that for the lower frequency, the fit is quite good. In this case we also show the long time extrapolation of the fit (dashed line). The long time departure is caused by the average density reduction due to drainage. At $f=37$ kHz the fit seems to deviate significantly for $t\gtrsim 100$ min, the experimental values being lower that those predicted by the fit and this is observed for all the high frequency measurements. This is surely caused by the breakdown of the nondissipative approximation made to obtain Eq. (23). Table I shows that for low f the fitted values of b approach the expected value $b\approx 0.026$ 1/min, confirming that we can apply the Biot theory to our low frequency results. On the other hand, the fitted values of a at low frequency give $E_{\mathrm{M}}\approx 60$ mN/m. In spite of the rather rough estimation of B, this value is in good agreement with those found in the literature for the Marangoni elastic constant in the large surfactant concentration limit [39].

TABLE I. Parameters of the fit $[c(t)/c_{\mathrm{w}}]^2$ given by Eq. (29). The fourth column presents the regression coefficients.

f (kHz)	a	b(min^{-1})	R_c
2	1.42 ± 0.01[a]	0.020 ± 0.001	0.985
5	1.33 ± 0.01	0.022 ± 0.001	0.999
37	1.01 ± 0.05	0.038 ± 0.005	0.977
63	1.04 ± 0.08	0.040 ± 0.006	0.961
84	1.03 ± 0.07	0.038 ± 0.006	0.959

[a]This frequency corresponds to a single experimental run, with $\langle\rho\rangle=0.071$ g/cm^3. ϕ and c_{w} are then corrected.

Before concluding this discussion, we will estimate the sound velocity of transverse waves. This is motivated by the experimental results of Sun *et al.* [18]. They effectively show that a foam can propagate as a transverse acoustic wave. We note that their measurements were performed in the frequency range 20–200 Hz. Compared to our measurements of the longitudinal velocity, they report a much lower transverse velocity, $c_{\mathrm{t}}=3.1\pm 0.4$ m/s. Unfortunately, they give little information about the foam characteristics. For example, the mean bubble size and the bubble size distribution are not reported. Nevertheless, they do mention the average density, 31 ± 4 kg/m^3. As the liquid they used is a mixture of distilled water and glycerine, we have approximately $\rho_l=1$ g/cm^3, so the average gas volume fraction is $\phi\approx 0.97$. They also indicate that their measurements were done with 1-h-old foams. On the other hand, Cohen-Addad *et al.* have studied the viscoelastic response of a coarsening foam [24], using Gillette shaving foams. They measured the temporal evolution of both elastic shear and loss moduli in the frequency range 0.04–3 Hz. For a foam age of 15 min, μ increases slowly with f from 400 to 500 Pa. By Eq. (23), we have $c_{\mathrm{t}}=\sqrt{\mu/\langle\rho\rangle}$. Considering that $\langle\rho\rangle\approx 76$ kg/m^3, we obtain that c_{t} increases slowly between 2.3 and 2.6 m/s with f. This value is very close to that found by Sun *et al.*; taking into account the differences of the foams, this may be a coincidence. The important point is that our estimation gives a good order of magnitude and we expect to find this value for our own foam samples. Finally, the difference in magnitude between the estimated values of c_{t} and the measured longitudinal sound velocity is very important. As noted before, it corresponds to a factor 700 between bulk and shear elastic moduli.

In conclusion, we have shown that frequency-dependent acoustic measurements can be used to probe foam coarsening. This is due to the high contrast of thermal and acoustic

properties at the liquid-gas interface within the foam, which leads to a dominant thermal dissipation. We have also observed that sound velocity depends on the structure of the foam even in the large wavelength regime. This is explained by considering the liquid matrix elasticity, which is related to Marangoni's elasticity. A simple model of foam structure, combined with the low frequency Biot theory, gives both good qualitative and quantitative agreement with our experimental results in the low frequency regime.

ACKNOWLEDGMENTS

We acknowledge Christophe Coste for useful comments on the manuscript. We also thank Vance Bergeron and Régis Wunenburger for discussions on the elasticity of liquid films. N.M. acknowledges Sergio Rica for many stimulating discussions. This work was financially supported by Chancellerie des Universités de Paris, France and Cátedra Presidencial en Ciencias (Chile).

[1] L. van Wijngaarden, J. Fluid Mech. **33**, 465 (1968).
[2] A. Crespo, Phys. Fluids **12**, 2274 (1969).
[3] G.K. Batchelor, in *Fluid Dynamics Transactions*, edited by W. Fiszdon, P. Kucharczyk, and W.J. Posnak (PWN-Polish Scientific, Warsaw, 1969), pp. 425–445.
[4] L. van Wijngaarden, Annu. Rev. Fluid Mech. **4**, 369 (1972).
[5] R.E. Caflisch, M.J. Miksis, G.C. Papanicolaou, and L. Ting, J. Fluid Mech. **153**, 259 (1985).
[6] E.L. Carstensen and L.L. Foldy, J. Acoust. Soc. Am. **19**, 481 (1947).
[7] F.E. Fox, S.R. Curley, and G.S. Larson, J. Acoust. Soc. Am. **27**, 534 (1955).
[8] J.D. Macpherson, Proc. Phys. Soc. London, Sect. B **70**, 85 (1957).
[9] E. Silberman, J. Acoust. Soc. Am. **29**, 925 (1957).
[10] K.W. Commander and A. Prosperetti, J. Acoust. Soc. Am. **85**, 732 (1989).
[11] C. Devin, J. Acoust. Soc. Am. **31**, 1654 (1959).
[12] A.I. Eller, J. Acoust. Soc. Am. **47**, 1469 (1970).
[13] A. Prosperetti, J. Acoust. Soc. Am. **61**, 17 (1977).
[14] A. Prosperetti, J. Fluid Mech. **222**, 587 (1991).
[15] J. Rubinstein, J. Acoust. Soc. Am. **77**, 2061 (1985).
[16] R.E. Caflisch, M.J. Miksis, G.C. Papanicolaou, and L. Ting, J. Fluid Mech. **160**, 1 (1985).
[17] Z.M. Orenbakh and G.A. Shushkov, Acoust. Phys. **39**, 63 (1993).
[18] Q. Sun, J.P. Butler, B. Suki, and D. Stamenović, J. Colloid Interface Sci. **163**, 269 (1994).
[19] F.I. Vafina, I.I. Gol'dfarb, and I.R. Shreiber, Akust. Zh. **38**, 260 (1992) [Sov. Phys. Acoust. **38**, 139 (1992)].
[20] I.I. Gol'dfarb, I.R. Shreiber, and F.I. Vafina, J. Acoust. Soc. Am. **92**, 2756 (1992).
[21] The Gillette Company, Gillette U.K. Ltd., London.
[22] D.J. Durian, D.A. Weitz, and D.J. Pine, Phys. Rev. A **44**, R7902 (1991).
[23] H. Hoballah, R. Holler, and S. Cohen-Addad, J. Phys. II **7**, 1215 (1997).
[24] S. Cohen-Addad, H. Hoballah, and R. Holler, Phys. Rev. E **57**, 6897 (1998).
[25] W.W. Mullins, J. Appl. Phys. **59**, 1341 (1986).
[26] A.B. Wood, *A Textbook of Sound* (Bell and Sons, London, 1944), pp. 360–363.
[27] K.F. Herzfeld, Philos. Mag. **9**, 752 (1930).
[28] M. Minnaert, Philos. Mag. **16**, 235 (1933).
[29] R.P. Feynman, R.B. Leighton, and M. Sands, *Lectures On Physics* (Addison-Wesley, Reading, MA, 1969), Vol. II.
[30] T.G. Leighton, *The Acoustic Bubble* (Academic Press, New York, 1994).
[31] L.D. Landau and E.M. Lifshitz, *Theory of Elasticity*, 3rd ed. (Pergamon Press, New York, 1986).
[32] For long aging times, the accumulation of a thin liquid layer on the transducer can induce changes on the acoustic transmission to the foam. However, once the acoustic pulse enters the foam, this liquid layer does not affect its propagation. Indeed, a liquid layer would affect the absolute values of $p_{\max}$ and τ_{fl}, but not their relative values with respect to changes of L.
[33] L.D. Landau and E.M. Lifshitz, *Fluid Mechanics*, 2nd ed. (Butterworth Heinemann, Oxford, 1987).
[34] P.M. Morse and K.U. Ingard, *Theoretical Acoustics* (Princeton University Press, Princeton, NJ, 1986).
[35] M.J. Miksis and L. Ting, Phys. Fluids **30**, 1683 (1987).
[36] R.J. Urick, J. Acoust. Soc. Am. **20**, 283 (1948).
[37] J.R. Allegra and S.A. Hawley, J. Acoust. Soc. Am. **51**, 1545 (1972).
[38] National Institute of Standards and Technology Chemistry WebBook, http://webbook.nist.gov/chemistry
[39] A.I. Rusanov and V.V. Krotov, Prog. Surf. Membr. Sci. **13**, 415 (1979).
[40] Y. Couder, J.M. Chomaz, and M. Rabaud, Physica D **37**, 384 (1989).
[41] D.L. Johnson, in *Frontiers in Physical Acoustics*, Proceedings of the International School of Physics "Enrico Fermi," Course XCIII, edited by D. Sette (North-Holland, Amsterdam, 1986), pp. 255–290.